06

Influence of shock-wave loading parameters on deformation and damage of a hollow steel cylinder

© V.O. Kopytskiy, A.Yu. Malakhov, I.V. Denisov, E.V. Petrov, F.F. Galiev, S.A. Seropyan

Institute of Structural Macrokinetics and Materials Science Problems, Russian Academy of Sciences, Chernogolovka, Russia
E-mail: kvo@ism.ac.ru

Received October 15, 2025
Revised January 17, 2026
Accepted January 19, 2026

This study examines the behavior of hollow cylinders manufactured from 08Kh18N10T corrosion-resistant steel with an internal Ni−Al powder compact barrier under dynamic shock-wave compression. The correlation between shock-wave parameters and the degree of cylinder collapse was quantified. The resulting deformation structures were characterized, revealing the presence of NiAl intermetallic compounds at anomalously large distances from the original compact location within the imploded cylinder.

Keywords: shock-wave loading, compression, spall cracks, localized shear bands, detonation speed, NiAl.

DOI: 10.61011/TPL.2026.05.63286.20528

It is known that as a result of natural and man-made disasters, load-carrying and protective structures can be subjected to heavy impacts, explosions and other impulse actions. As a result of such actions, structural materials undergo plastic deformation when exposed to elastoplastic or shock waves. The influence of pulse loading on the properties of structural materials is studied using shock wave loading (SWL) methods [1–4].

SWL L induces intense plastic deformation of a material's crystal structure due to the high pressures generated by the explosive charge. Cylindrical shells made of various metals are often used to study the SWL effect on materials [5–8]. Full collapse of cylindrical shells without fracture is achieved through optimum selection of explosive charge parameters (weight, detonation velocity and pressure) and experimental assembly configuration. Compliance of the load pulse with the material's dynamic ultimate strength is a critical condition: when the pulse is insufficient, the cylinder doesn't collapse completely, and when the pulse is excessive, the cylinder fractures. To ensure controlled collapse without loss of integrity, charge parameters shall be selected such that the explosive energy is completely absorbed by the cylinder material by the time when the deformation process is completed [7,8].

In [9], the authors used SWL of cylindrical vials to initiate self-propagating high-temperature synthesis (SHS) and to perform extrusion of the Ni−Al powder mixture. In [10–13], SWL was used solely for compacting of various powders. Studies [10–14] have shown that powder mixtures in high temperature and pressure conditions typical of SWL and SHS processes can form intermetallic compounds, with NiAl being the most widespread one, as it has high melting temperature (1638 °C), hardness, heat resistance, oxidation resistance and corrosion resistance.

The relevance of this study is in the importance of SWL parameter optimization to minimize the failure rate and improve structural material strengthening, and the potential of using NiAl-type intermetallic systems for modification of properties of steel components under dynamic loads.

Thus, according to the existing data, it could be pointed out that no special focus has been made on the deformed material structure during compaction or shock-wave synthesis of powder mixtures in cylindrical vials. The effect of a barrier in the form of exothermic mixture of powders (for example, Ni−Al) on collapse of a hollow cylinder hasn't been addressed either. Considering the foregoing and according to the previous findings of [9], this study set out to evaluate the effect of SWL parameters on the formation of deformed structures, and to determine the nature of deformation processes taking place in the microstructure and macrostructure of a hollow cylinder with compacted powder mixture inside after exposure to SWL. For this, macrostructure and microstructure were examined in various areas of the reduced cylinder.

The effect of SWL parameters on the formation of the hollow cylinder structure was studied using two experimental setups (Figure 1). Hollows cylinders (length 70 mm) with a wall thickness of 2 mm and a bore of 10 mm were made of steel 08X18H10T. The first setup used ammonite 6ZhV (detonation velocity 3750 m/s, explosive detonation pressure 3.5 GPa) as an explosive substance (ES) (Figure 1, *a*). The second setup (Figure 1, *b*), in addition to ammonite, used a mixture of microporous ammonium nitrate and diesel fuel at the ratio of 96:4 (detonation velocity 3150 m/s, explosive detonation pressure 1.88 GPa). The powder mixture consisted of nickel powder PNK-UT3 (particle size $d \sim 18\,\mu$m) and aluminum powder ASD-1 ($d \sim 20\,\mu$m) in an equimolar ratio. Initial powders were pressed at a uniaxial pressure in a steel mold to prepare cylindrical samples with a relative density of about 65−70 % of the maximum possible theoretical value. Compacted pellets 10 mm in diameter and 10 mm in height were placed

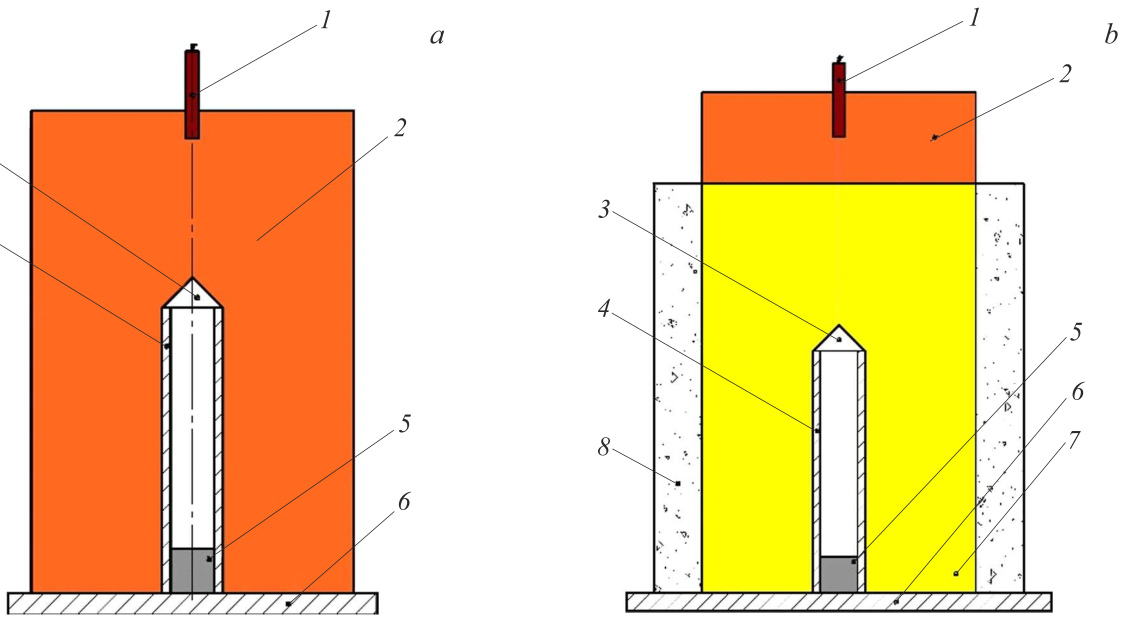

Figure 1. Experimental setup. (*a*) — experiment 1, (*b*) — experiment 2. *1* — detonator, *2* — ammonite 6ZhV, *3* — fairing, *4* — cylinder, *5* — Ni–Al, *6* — support, *7* — igdanite, *8* — sand.

at the bottom of a hollow cylinder. For the first and second setups, the explosive charge diameter was 70 mm and 116 mm, respectively. The second setup also used an external sand layer to reduce the explosive's ability to accelerate by means of shock wave energy dissipation.

Experiments have shown that the compacted mixture affected the deformation behavior of a hollow steel cylinder in the system. Test cross-sections of reduced samples are shown in Figure 2. Three cross-sections were examined for each sample: I — upper cross-section at the beginning of reduction, II — middle cross-section in the center of the sample, III — lower cross-section at the end of reduction, immediately above the compact.

Figure 2, *a* shows the cross-section images of sample No 1. Cross-section I has four radial cracks bent in the same direction and extended to the cylinder's free surface, which have a deformation shear nature. A grid of localized deformation bands was detected in the central region around the 0.2 mm opening. Curvature and orientation of cracks prove a significant role of shear deformation induced by asymmetric action of detonation wave. Dispersed particles were detected on cross-section II inside the 0.8 mm opening and, according to the further energy-dispersive spectroscopy (EDS) analysis, showed anomalously high concentration of Ni and Al. Radial cracks originating from the 1.6 mm opening, but not reaching the free surface, were also identified on cross-section III. Cracking is associated with tensile stresses induced by interaction of counterpropagating unloading waves [15,16].

Figure 2, *b* shows cross-sections of sample No 2. Cross-section I has no opening, there are only traces of severe plastic deformation in the axial zone with typical localization bands. A 0.3 mm opening with radial cracks, which also demonstrate a bending trend, was detected on cross-section II. During deformation localization, spallation cracks often propagate along localized shear bands oriented at angles close to 45° to the maximum tangent stress direction. There are no Ni/Al-enriched particles in the internal space. An opening with a mean diameter of 1.0 mm with deformed material inclusions are observed in cross-section III. Unlike sample No 1, there are no clearly pronounced cracks exposed on the outer surface, and opening diameters on all cross-sections are much smaller. Wall thickness in both cases increased by a factor of 2.5 (from 2 mm to 5 mm). Despite the presence of a barrier, the mode of failures meets the pattern observed in reduction of cylinders without a barrier with similar loading parameters [17], indicates the dominating role of shock impact parameters over the barrier effect in these experimental conditions.

Figure 3 and table show the EDS analysis data for products detected in the opening on cross-section II of sample No 1. Different Ni/Al ratio is observed in various particles, and there is also iron from the cylinder material, which is indicative of vigorous mechanical stirring. EDS analysis and X-ray diffraction analysis (XPA) (Figure 4), which have shown the presence of NiAl and Ni_3Al phases, prove that there are traces of NiAl intermetallic compounds, regardless of the fact that the cross-section is 20 mm away from the compacted Ni–Al mixture and convergence of cylinder walls occurs before the time when compression reaches the barrier in the form of compact. However, mass transfer occurs during compression due to release of powder particles under the shock wave action, interaction between the particles and deformed steel matrix, and possible melting caused by local adiabatic heating. Possible formation of intermetallic compounds as a result of SWL has

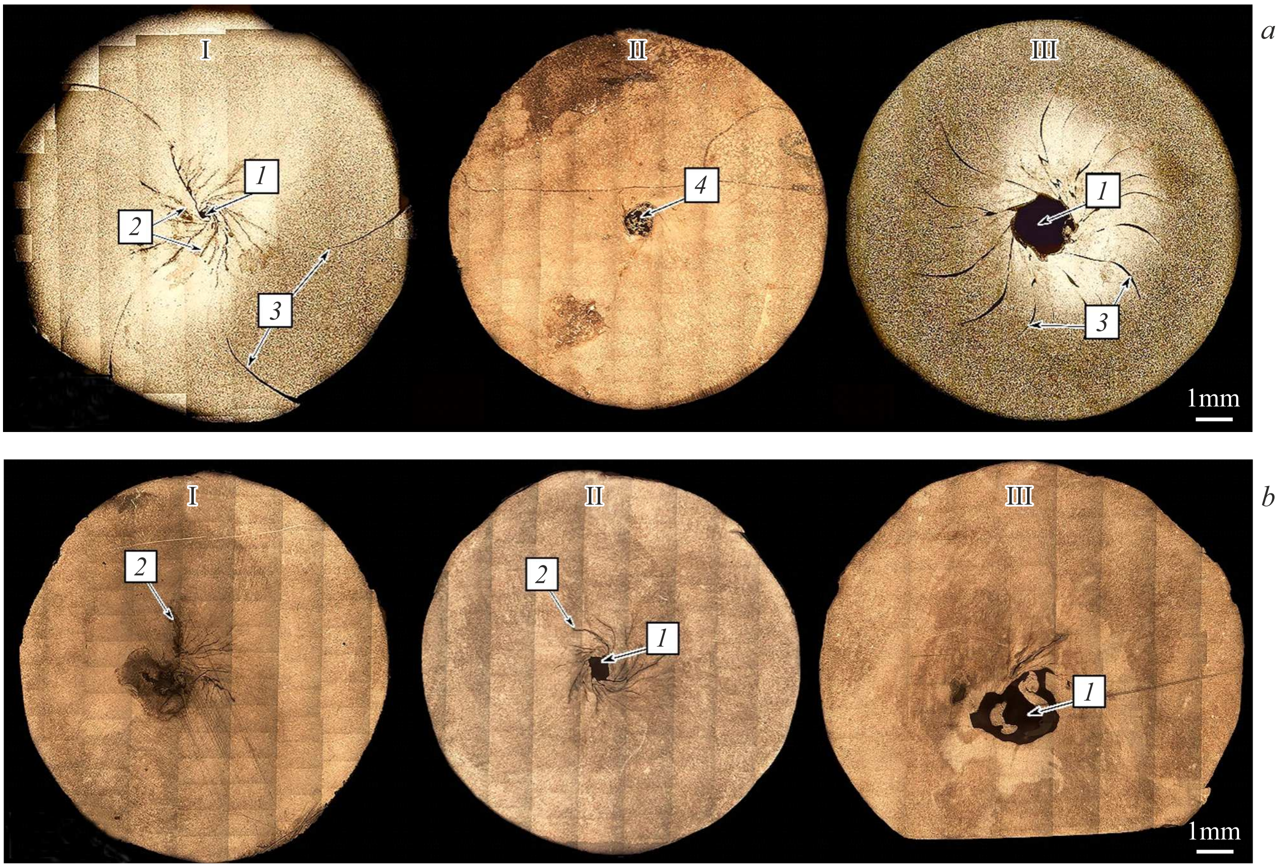

Figure 2. Optical images of cross-sections of samples No 1 (*a*) and 2 (*b*). *1* — opening, *2* — localized deformation bands, *3* — radial cracks, *4* — NiAl. Cross-sections are marked by Roman numerals (explained in the text).

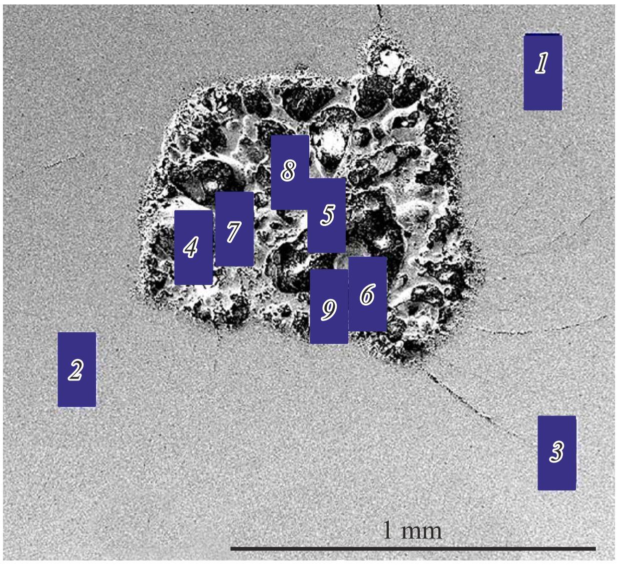

Figure 3. Scanning electron microscopy image of the structure of opening in cross-section II of sample No 1. Energy-dispersive spectra are marked by numbers from *1* to *9*.

been also proved previously in [9]. Determination of NiAl on other cross-sections within cylinders is the objective of further studies.

Reduction of hollow stainless steel cylinders caused formation of almost solid cylindrical samples. Metallographic examination has detected that sample No 1 had a higher spallation failure rate and larger diameters of remaining openings than sample No 2. Experiment results have shown that when a hollow cylinder was exposed to creeping detonation wave, a shock wave propagating inside the material was induced. The shock wave front is followed by unloading wave that induces tensile stresses in the pre-compressed material. The observed difference in the degree of compression along the cylinder axis is explicitly associated with different SWL parameters. Material's failure rate (spallation cracks) is formed predominantly at the unloading stage where the action of compressive stresses stops [15,16].

Thus, it has been found that an increase in the impulse loading time by placing the experimental assembly into a sand layer led to a significant reduction of material failure rate. It has been shown that the outer surface of sample No 2 with an increased loading time remained integral, and the number of radial spallation cracks in the paraxial region decreased. It has been found that even when

EDS data (in at.%) by spectra marked in Figure 3

Spectrum number	Al	Ti	Cr	Fe	Ni
1	1.51	1.38	18.64	68.43	10.04
2	1.42	1.21	19.63	68.35	9.39
3	1.62	1.20	18.01	68.85	10.32
4	13.95	1.59	8.22	66.88	9.36
5	1.07	0.36	18.43	70.71	9.43
6	33.49	0.82	5.74	19.64	40.31
7	35.42	0.57	21.38	39.38	3.25
8	57.59	0.14	16.97	24.42	0.88
9	50.03	0.19	11.97	25.62	12.19

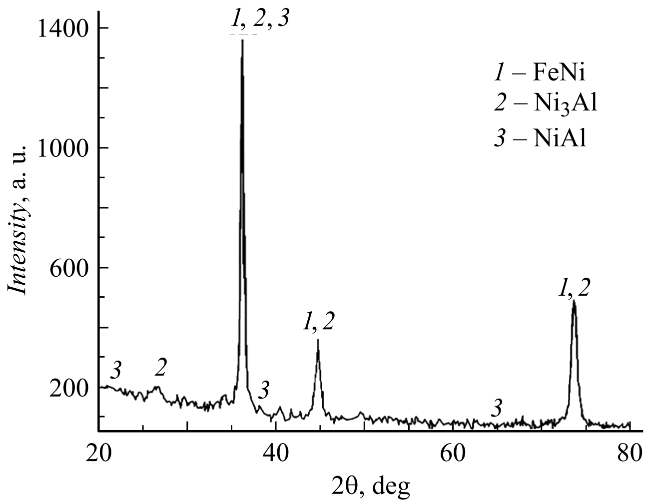

Figure 4. Diffraction pattern (XPA) in central region of cross-section II of sample No 1.

the impulse action was reduced in that conditions, full reduction of the cylinder didn't occur in cross-sections near the compact: openings with reduced diameter remained. Anomalous distribution of NiAl synthesis products has been also detected at a distance up to 20 mm from the initial compact position.

Observed anomalous distribution of NiAl synthesis products indicates complex physical and chemical processes requiring additional study of intermetallic compound migration and synthesis mechanisms. The findings are important for the development of methods for material structure and property management during dynamic loading.

Funding

The study was carried out under the state order of the Institute of Structural Macrokinetics and Materials Science Problems (No 125021201986-5).

Conflict of interest

The authors declare no conflict of interest.

References

[1] I.G. Brodova, V.I. Zel'dovich, I.V. Khomskaya, Phys. Met. Metallogr., **121** (7), 631 (2020). DOI: 10.1134/S0031918X20070029

[2] S. Yu, G. Zhang, H. Wu, Z. Wang, J. Yao, Q. Sun, M. Wang, Y. He, Eng. Struct., **285**, 115986 (2023). DOI: 10.1016/j.engstruct.2023.115986

[3] S.V. Razorenov, A.S. Savinykh, G.V. Garkushin, R.F. Muftakhetdinova, I.V. Khomskaya, G.A. Yakovlev, V.A. Khotinov, V.I. Grokhovsky, Tech. Phys., **69** (6), 803 (2024). DOI: 10.61011/TP.2024.06.58822.87-24

[4] I.A. Cherepanov, A.S. Savinykh, G.V. Garkushin, S.V. Razorenov, Tech. Phys., **69** (1), 119 (2024). DOI: 10.61011/JTF.2024.01.56910.247-23.

[5] S.N. Buravova, E.V. Petrov, A.S. Shchukin, Combust. Explos. Shock Waves, **52** (5), 613 (2016). DOI: 10.1134/S0010508216050129

[6] E.A. Kozlov, S.A. Brichikov, D.S. Boyarnikov, D.P. Kuchko, A.A. Degtyarev, Phys. Met. Metallogr., **112** (4), 389 (2011). DOI: 10.1134/S0031918X11040259

[7] V.I. Zel'dovich, N.Yu. Frolova, A.E. Kheifets, I.V. Khomskaya, A.A. Degtyarev, E.V. Shorokhov, E.B. Smirnov, S.M. Dolgikh, A.V. Koval', Combust. Explos. Shock Waves, **55** (4), 456 (2019). DOI: 10.1134/S0010508219040129.

[8] A.V. Koval', I.G. Shirinkina, A.N. Petrova, I.G. Brodova, E.B. Smirnov, E.V. Shorokhov, Combust. Explos. Shock Waves, **55** (4), 447 (2019). DOI: 10.1134/S0010508219040117

[9] A. Malakhov, D. Shakhray, I. Denisov, F. Galiev, S. Seropyan, Materials, **15** (17), 6062 (2022). DOI: 10.3390/ma15176062

[10] O.V. Ivanova, S.A. Zelepugin, Appl. Mech. Mater., **770**, 174 (2015). DOI: 10.4028/www.scientific.net/AMM.770.174

[11] N.A. Adamenko, L.N. Ignatieva, G.A. Zverev, G.V. Agafonova, V.A. Mashchenko, J. Fluor. Chem., **249**, 109852 (2021). DOI: 10.1016/j.jfluchem.2021.109852

[12] S.A. Zelepugin, O.V. Ivanova, A.S. Yunoshev, A.S. Zelepugin, Lett. Mater., **5** (4), 468 (2015). DOI: 10.22226/2410-3535-2015-4-468-472

[13] K.L. Olney, P.H. Chiu, A. Higgins, M. Serge, T.P. Weihs, G. Fritz, A. Stover, D.J. Benson, V.F. Nesterenko, J. Phys.: Conf. Ser., **500**, 132002 (2014). DOI: 10.1088/1742-6596/500/13/132002

[14] M. Sun, C. Li, X. Zhang, X. Hu, X. Hu, Y. Liu, Materials, **11** (11), 2267 (2018). DOI: 10.3390/ma11112267

[15] S.N. Buravova, E.V. Petrov, Forces Mech., **3**, 100015 (2021). DOI: 10.1016/j.finmec.2021.100015

[16] A.F. Belikova, S.N. Buravova, Yu.A. Gordopolov, Tech. Phys., **58** (2), 302 (2013). DOI: 10.1134/S1063784213020035

[17] V.F. Nesterenko, M.P. Bondar', Combust. Explos. Shock Waves, **30** (4), 500 (1994). DOI: 10.1007/BF00790157

Translated by E.Ilyinskaya